Biochemical Pharmacology 83 (2012) 616–626

Contents lists available at SciVerse ScienceDirect

Biochemical Pharmacology

journal homepage: www.elsevier.com/locate/biochempharm

Inhibition of Rho kinases increases directional motility of microvascular endothelial cells

Johannes Breyer [a], Jana Samarin [a,1], Margot Rehm [a], Lena Lautscham [b], Ben Fabry [b], Margarete Goppelt-Struebe [a,*]

[a] Department of Nephrology and Hypertension, Universität Erlangen-Nürnberg, Loschgestrasse 8, 91054 Erlangen, Germany
[b] Department of Physics, University of Erlangen-Nuremberg, Henkestrasse 91, 91052 Erlangen, Germany

ARTICLE INFO

Article history:
Received 19 October 2011
Accepted 8 December 2011
Available online 16 December 2011

Keywords:
Microvascular endothelial cells
Rho kinase
ROCK2
Connective tissue growth factor
Actin cytoskeleton
Cell motility

ABSTRACT

Rho kinases are major regulators of actin cytoskeletal organization and cell motility. Depending on the model system, inhibitors of Rho kinases (ROCK) have been reported to increase or decrease endothelial cell migration. In the present study we investigated the effect of Rho kinase inhibitors on microvascular endothelial cell migration with a special focus on the isoform ROCK2.

Migration of microvascular endothelial cells was analyzed in a wound-healing, a spheroid-on-collagen migration assay and in cells embedded in collagen-1 gels. The non-selective Rho kinase inhibitor H1152 was compared to the selective ROCK2 inhibitor SLX2119 and to siRNA knock down.

Non-selective inhibition of Rho kinases decreased cell-spanning F-actin fibers, loosened cell–cell contacts visualized by VE cadherin staining, and reduced cell–matrix interactions as shown by reduced Hic-5 expression in focal contacts. Rho kinase inhibitors facilitated directed migration of endothelial cells away from spheroids on fibronectin-coated plates and in collagen-1 gels. By contrast, migration of firmly attached endothelial cells, resembling intact vessels, was not promoted by Rho kinase inhibition. Selective inhibition of ROCK2 mimicked the cytoskeletal effects of H1152 and also increased cell motility, although to a lesser extent.

In summary, Rho kinase inhibition enhanced the migration and cytoskeletal restructuring preferentially in freshly attached endothelial cells. ROCK2 may be a potential target to manipulate endothelial cell migration after vessel injury.

1. Introduction

Rho-associated coiled coil forming protein kinases (ROCK) are important downstream mediators of the small GTP-binding protein RhoA. They regulate actin stress fiber formation and cell contraction and thereby affect cell shape, adhesion, and migration [1,2]. Furthermore, by interacting with other signaling pathways or by shifting the equilibrium between globular and filamentous actin, Rho kinases affect gene expression [3]. Rho kinases are involved in a number of human disorders, and several pharmacological inhibitors have been developed and clinically tested [4,5]. Most of the inhibitors developed thus far inhibit both Rho kinase isoforms, ROCK1 and ROCK2 [6]. Of those, fasudil (HA1077) shows potent vasodilatory effects and was approved for clinical use in Japan for the treatment of patients with cerebral vasospasm as a result of subarachnoid hemorrhage [7]. Since then, Rho kinases have emerged as potential targets for the treatment of vascular diseases, hypertension and atherosclerosis [8–12].

Activated Rho kinases contribute to endothelial dysfunction by inhibiting expression of endothelial NO synthase and NO synthesis,

Abbreviations: H1152, (*S*)-(+)-2-methyl-1-[(4-methyl-5-isoquinolinyl)sulfonyl]-homopiperazine; BrdU, 5-bromo-2′-deoxyuridine; CTGF, connective tissue growth factor; DMOG, dimethyl-oxalylglycine; HUVEC, human umbilical vein endothelial cell; LPA, lysophosphatidic acid; MLC, myosin light chain; MYPT, MLC phosphatase; ROCK, Rho kinase, small G protein Rho-associated kinase; VEGF, vascular endothelial growth factor; Y-27632, (+)-(*R*)-*trans*-4-(1-aminoethyl)-*N*-(4-pyridyl) cyclohexanecarboxamide dihydrochloride.

* Corresponding author at: Department of Nephrology and Hypertension, Universitätsklinik Erlangen, Friedrich-Alexander Universität Erlangen-Nürnberg, Loschgestrasse 8, D-91054 Erlangen, Germany. Tel.: +49 09131 8539201; fax: +49 09131 8539202.

E-mail addresses: hannes.breyer@gmx.de (J. Breyer), Samarin@gmx.de (J. Samarin), Margot.Rehm@uk-erlangen.de (M. Rehm), lena.lautscham@googlemail.com (L. Lautscham), Ben.Fabry@biomed.uni-erlangen.de (B. Fabry), margarete.goppelt-struebe@uk-erlangen.de (M. Goppelt-Struebe).

[1] Present address: Institute of Pathology, University of Heidelberg, Im Neuenheimer Feld 220/221, 69120 Heidelberg, Germany.

0006-2952/$ – see front matter © 2011 Elsevier Inc. All rights reserved.
doi:10.1016/j.bcp.2011.12.012

to inflammation by activation of NF-kB, and to endothelial barrier disruption by microtubule and actin rearrangements [13–15].

Effects of Rho kinase inhibitors on vascular remodeling and endothelial motility have been analyzed in various assays. Increased sprouting activity was detected in human umbilical vein endothelial cells (HUVECs) treated with Rho kinase inhibitors or siRNA directed against ROCK1 or ROCK2 [16,17]. By contrast, others reported reduced HUVEC migration in the presence of Rho kinase inhibitors [18], and reduced migration and structure formation of bovine retinal and human foreskin microvascular endothelial cells [19,20]. The discrepancies between these reports remain unclear as different types of endothelial cells and different *in vitro* model systems were used.

The Rho kinase isoforms ROCK1 and ROCK2 are highly homologous and share major down stream targets such as myosin light chain (MLC) or MLC phosphatase (MYPT) [4]. Nevertheless, there is increasing evidence of isoform specific effects in different cell types, *e.g.* fibroblasts [21,22] or keratinocytes [23]. ROCK2 activation was linked to the expression of cell adhesion molecules upon stimulation of HUVEC with lysophosphatidic acid (LPA) [14], and to VEGF-driven angiogenesis [24]. These data suggest that pharmacologic inhibition of one or the other Rho kinase isoform may be sufficient to obtain relevant therapeutic results. Thus far, however, only few isoform-specific inhibitors have been developed, all of them being directed against ROCK2, among them SLX-2119 [25]. To assess the role of ROCK2 in microvascular endothelial cell motility in different *in vitro* model systems, we used the selective inhibitor SLX-2119 as well as selective inhibition of ROCK2 by siRNA, and compared it to the non-selective inhibitor H1152.

Our data provide evidence for an increase in endothelial directional cell motility when both Rho kinase isoforms are inhibited. Depending on the model system, a somewhat smaller increase in cell motility was also achieved by selective inhibition of ROCK2. We also show that the effect of ROCK inhibition was dependent on the adhesion status of the endothelial cells: enhanced cell migration was only seen when the cells were not yet firmly attached to the extracellular matrix.

2. Materials and methods

2.1. Cell culture

The murine glomerular microvascular endothelial cell line (glEND.2) was kindly provided by R. Hallmann (Muenster, Germany). Cells were characterized by positive staining for typical endothelial cell markers MECA-32 and CD-31, and the lack of staining of mesangial cell markers such as α-smooth muscle actin and α8-integrin, as well as epithelial cells markers such as WT-1 and cytokeratin [26]. Cells were cultured at 37 °C and 7.5% CO_2 in Dulbecco's modified Eagle's medium (DMEM) containing 10% FCS and routinely split in a 1:5 ratio as described previously [27].

2.2. Western blot analysis

For inhibitor experiments, glEND.2 cells were pretreated for 30 min with H1152 (0.75–1.5 μM) or SLX2119 (1 μM) at 37 °C, followed by incubation with LPA (10 μM) at 37 °C for the indicated times. Cells were lysed in buffer containing 50 mM Hepes (pH 7.4), 150 mM NaCl, 1% Triton X-100, 1 mM EDTA, 10% glycerol, protease inhibitor cocktail Complete (Roche Diagnostics GmbH, Mannheim, Germany) and 2 mM Na_3VO_4 for the detection of connective tissue growth factor (CTGF) in cellular homogenates. For the detection of pMYPT, cells were lysed in buffer containing phosphate buffered saline (PBS), 4% SDS and 1 mM NaF. In order to detect VE-cadherin, cells were lysed in buffer containing 6.65 M urea, 10% glycerol, 1% SDS, 10 mM Tris (pH 6.7) and 2.5 mM DDT.

Proteins were separated by SDS-PAGE and transferred onto PVDF membranes by standard protocols. The following antibodies were used: goat polyclonal anti-CTGF (SC-14939), rabbit polyclonal anti-vinculin (SC-5573), rabbit anti-ROCK2 (SC-5561), peroxidase-conjugated donkey anti-goat IgG (SC-2020) and goat anti-rat IgG (SC-2006, Santa Cruz Biotechnology, Heidelberg, Germany). Rabbit anti-pMYPT (Thr853) (#4563) was from Cell Signalling (Danvers, MA, USA). Rat anti-VE-cadherin (#14-1441) was obtained from eBioscience (San Diego, CA, USA), mouse monoclonal anti-tubulin (T0198) from Sigma (Munich, Germany), sheep anti-mouse IgG (NA931V) and donkey anti-rabbit IgG (NA934V) secondary antibodies from Amersham Biosciences (Freiburg, Germany).

Immunoreactive proteins were visualized by the enhanced chemiluminescence detection system (ECL-Plus, Amersham). Immunoreactive bands were quantified using the luminescent image analyzer (LAS-1000 Image Analyzer, Fujifilm, Berlin, Germany) and AIDA 4.15 image analyzer software (Raytest, Berlin, Germany). To correct for equal loading and blotting, all blots were redetected with antibodies directed against vinculin or tubulin. For quantification purposes, the ratio of the specific protein band and a control protein was calculated.

2.3. Immunocytochemistry

glEND.2 cells were fixed with 3.5% paraformaldehyde in Dulbecco's PBS (140 mM NaCl, 2.68 mM KCl, 1.47 mM KH_2PO_4 and 8.1 mM Na_2HPO_4) for 10 min, or for BrdU-staining with 2.3 M HCl in 99.9% C_2H_5OH for 24 h. Afterwards, cells were permeabilized by 0.2% Triton X-100 in PBS for 10 min. Cells were incubated at 4 °C with primary antibodies against Hic-5 (1:200, #611165, BD Biosciences, Bedford, MA, USA) or VE-cadherin (1:25, #14-1441, eBioscience, San Diego, CA, USA) or BrdU (1:20, #347580, BD Bioscience, Bedford, MA, USA) overnight, and with secondary antibody (1:500, Alexa Fluor® 488 anti-mouse A21202 or 488 anti-rat A11006, Molecular Probes, Eugene, OR, USA) for 45 min. F-actin was stained by incubation with Alexa Phalloidin 547 (FP-AZ0330) or 505 (FP-AZ0130, Interchim SA, Montlucon, France) for 20 min. Nuclei were stained with Hoechst (Sigma–Aldrich, St. Louis, MO, USA). After mounting, slides were viewed using a Nikon fluorescence microscope. Digital images were recorded using Spot imaging software (Diagnostic Instruments, MI, USA).

All stainings shown are representative for at least 3 independent experiments.

2.4. siRNA transfection

To down-regulate ROCK-2 expression, endothelial cells (glEND.2) were transfected with ROCK-2 siRNA, 50 nM (#1: sense 5′-GCA-GCA-CGG-UUA-AGA-AAA-A-3′; #2: sense 5′-GGA-GAU-UAC-CUU-ACG-GAA-A-3′), or CTGF siRNA (sense 5′-GUG-AGA-ACG-UUA-UGU-CAU-3′) or an irrelevant siRNA (5′-GGA-UGG-CAU-CUC-GGA-GCU-C-3′) 3 h after seeding using HiPerFect (QIAGEN GmbH, Hilden, Germany) according to the manufacturer's instructions. Experiments were performed 48 h after transfection.

2.5. Migration assays

Lateral migration assays were performed as described in Ref. [28].

Cell spheroids (400 cells per spheroid) were created using the hanging drop method [29]. In brief, cells were suspended in DMEM with 0.24% methylcellulose. Cell suspension drops (400 cells/25 μl) were deposited onto the underside of the lid of a tissue culture dish. The lid was inverted and incubated overnight at 37 °C.

For the spheroid migration assay, single spheroids were deposited separately on fibronectin-coated glass plates and stimulated as described in Section 3. To determine cell proliferation, spheroids were incubated with BrdU for the last 3 h. After 24 h, cells were fixed with 3.5% paraformaldehyde. F-actin and nuclei were stained for quantification purposes to determine area and cell numbers of at least 6 spheroids per experimental group using ImageJ software.

Collagen-1 gel matrices were prepared by mixing a collagen solution (2 mg/ml collagen-1 in Earle's BSS, pH 7.2–7.6) with methylcellulose (1% in DMEM with 20% FCS) at a ratio of 1:1. 300 μl of the matrix per well were allowed to polymerize for 30 min at 37 °C. Afterwards, 30–50 spheroids were mixed with unpolymerized matrix solution and plated on top of the polymerized collagen-1 gel. Spheroids were incubated at 37 °C with 7.5% CO_2 and observed for 6 days. Phase contrast images were taken of 10 spheroids each well every day. Sprout length and number of intact sprouts from 8 to 10 spheroids per experimental group and experiment was measured using ImageJ software.

2.6. Live cell imaging

Cell spheroids were monitored with an inverted microscope (Leica DMI3000B) in phase contrast mode using a 20 × 0.4 NA objective with a 0.5× video coupler. The microscope was equipped with an incubation chamber to maintain the spheroids at 37 °C and 7.5% CO_2. Images were taken every 350 s over a time period of up to 24 h. Cells moving out from the spheroid bodies were tracked with a custom image processing software written in MatLab. Starting from the last image of a sequence, a square region measuring 7 μm × 7 μm was manually selected around the center of each cell. Going back in time, the movement of this region in all the preceding images was then obtained from a cross correlation analysis until the cell could no longer be tracked either because it merged with the spheroid body, or it underwent a cell division.

From the cell trajectories, the mean square displacement (MSD) was calculated [30]. As the MSD between cells shows a log-normal distribution, the geometric mean and geometric standard error were computed. We also computed for the trajectory of each cell a power-law fit of the form $MSD = D \times (\Delta t/\Delta t_0)^{\beta}$, with D denoting the apparent diffusivity (the MSD at the reference time $\Delta t_0 = 1$ min), and β denoting the power-law exponent. The time interval Δt ranged from 350 s to 930 min. D characterizes the speed of cell movements at short time intervals, and β characterizes the persistence of cell movement at long time intervals [31]. β typically ranges from a value of 1 for randomly migrating cells to a value of 2 for persistent, ballistically migrating cells [31].

For each trajectory, we also computed the turning angle of cell movement between subsequent time intervals ranging again from 350 s to 930 min [31]. A mean of the absolute value of the turning angle around zero characterizes persistent motion, and a value of 90° characterizes random motion.

From the position of the cells we also computed the smallest circle enclosing all cells of a spheroid by finding the maximum circumcircle of any combination of three cell positions. The radius of the smallest circle enclosing all cells *versus* time (from 350 s to 930 min) characterizes the motion of the outermost cells of the spheroid.

2.7. Data analysis

Data are presented as means ± SD or SEM of n independent experiments as detailed in the legends. If not indicated otherwise, an ANOVA with Tukey–Kramer multiple comparison or a Dunnett *post hoc* test was used to compare multiple measurements (Prism GraphPad Software, La Jolla, CA, USA). Student's t-test was used to compare two groups. A p-value < 0.05 was considered significant.

2.8. Materials

Cell culture materials were purchased from PAA Laboratories (Pasching, Austria). The following biochemicals were used: lysophosphatidic acid and 5-bromo-2′-deoxyuridine, (BrdU) (Sigma–Aldrich, Munich, Germany), dimethyl-oxalylglycine (DMOG, Axxora, Lörrach, Germany); (*S*)-(+)-2-methyl-1-[(4-methyl-5-isoquinolinyl)sulfonyl]-homopiperazine [32] (ALX-270-423-M001, Alexis Biochemicals, Grünberg, Germany), collagen-1 (#5005-B Pure Col, 3 mg/ml, Advanced Bio Matrix, San Diego, CA, USA), methylcellulose 4000 (Fluka, Sigma–Aldrich, Munich, Germany). SLX2119 was kindly provided by Surface Logix, Brighton, MA, USA.

3. Results

3.1. Inhibition of ROCK2 is sufficient to reduce p-MYPT phosphorylation

To characterize Rho kinase inhibitors in glEND.2 microvascular endothelial cells, phosphorylation of MYPT, a subunit of myosin light chain phosphatase and direct target of Rho kinases, was detected by Western blot analysis. Incubation of the cells with the non-selective inhibitor of both Rho kinase isoforms H1152 or the selective ROCK2 inhibitor SLX2119 for 2 h inhibited phosphorylation of MYPT in a concentration dependent manner (Fig. 1A). Concentrations of 1 μM SLX2119 and 1.5 μM H1152 inhibited phosphorylation of MYPT by about 80% and were chosen for further experiments.

Downregulation of ROCK2 was achieved with two different siRNAs, which had no effect on ROCK1 (Fig. 1B). ROCK2 protein expression was reduced to 44 ± 16%, mean ± SD of $n = 6$ experiments with 2 different siRNAs each. Specific downregulation of ROCK2 resulted in a marked decrease in MYPT phosphorylation. For comparison, cells treated with a non-functional siRNA were incubated with H1152 (Fig. 1B).

As a functionally relevant target protein we measured the expression of connective tissue growth factor, a matricellular protein that is critically dependent on RhoA–ROCK signaling and alterations of the actin cytoskeleton [33,34]. CTGF synthesis was stimulated in glEND.2 cells using lysophosphatidic acid [35] (Fig. 1C). Non-selective ROCK inhibition with H1152 reduced basal CTGF expression and prevented CTGF induction by LPA above basal levels of control cells. Selective targeting of ROCK2 by the selective inhibitor SLX2119 showed a tendency to reduced CTGF expression but did not reach statistical significance. Higher concentrations of SLX2119 did not further reduce CTGF induction (data not shown). Short term inhibition of one Rho kinase isoform was thus not sufficient to interfere with CTGF expression. By contrast, long term reduction of ROCK2 expression by specific siRNAs significantly reduced CTGF protein expression, even though the siROCK2 knockdown was not complete (Fig. 1D).

3.2. Inhibition of Rho kinases does not affect lateral migration of microvascular endothelial cells

In previous experiments we have shown that inhibitors of Rho kinases strongly stimulated lateral migration of epithelial cells [36]. Accordingly, we used wound healing scratch assays and barrier assays to analyze lateral migration of glEND.2 cells. Unlike the scratch assay, the barrier assay keeps the extracellular matrix intact. Over a time period of 24 h, glEND.2 cells very slowly moved into the open space (Fig. 2A). To induce pro-migratory factors such as VEGF, cells were incubated with DMOG (1 mM), which by

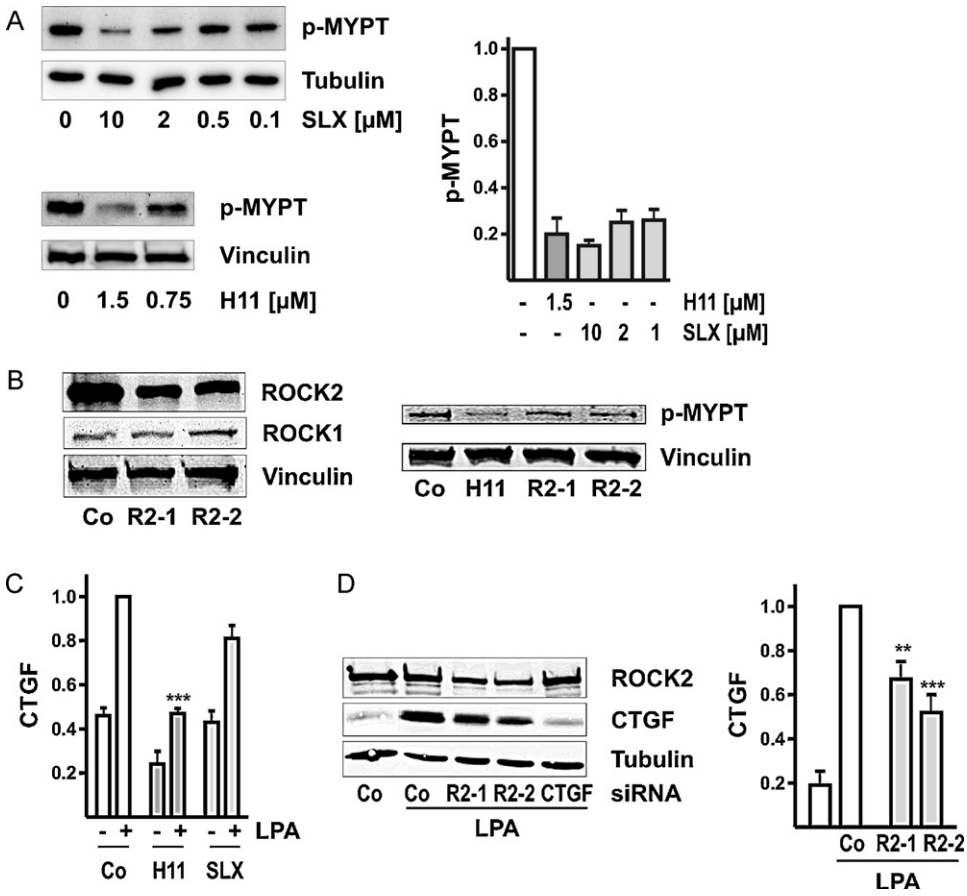

Fig. 1. Characterization of Rho kinase inhibitors in microvascular endothelial cells. (A) glEND.2 cells were incubated with Rho kinase inhibitors H1152 or SLX2119 for 2 h as indicated. Phosphorylation of MYPT at threonine 853 was detected by Western blotting. The ratio p-MYPT to house keeping protein was determined densitometrically. To compare different experiments, expression in control cells was normalized to 1. Mean ± SD of 3 experiments are summarized in the graph. (B) glEND.2 cells were transfected with two different siRNAs selective for ROCK2 (R2-1, R2-2) or control siRNA. Expression of ROCK1, ROCK2 and p-MYPT was detected by Western blotting. Blots representative of 3 independent experiments are shown. (C) glEND.2 cells were treated with H1152 (1.5 μM) or SLX2119 (1 μM) for 30 min and then further incubated with LPA (10 μM) for 2 h. Cell-associated CTGF was detected by Western blotting. Expression of CTGF was related to tubulin or vinculin expression, and normalized to LPA-stimulated cells. Data are means ± SD of 3 independent experiments; ***Indicate significant ($p < 0.001$) differences compared to LPA-stimulated cells. (D) glEND.2 cells were treated with siRNA against CTGF, control siRNA (Co) or siRNAs against ROCK2. ROCK2 and CTGF were detected by Western blotting. Expression of CTGF was related to tubulin or vinculin expression, and normalized to LPA-stimulated cells. The graph summarizes the data of 4 independent experiments; means ± SD, **$p < 0.01$, ***$p < 0.001$ compared to LPA-stimulated cells.

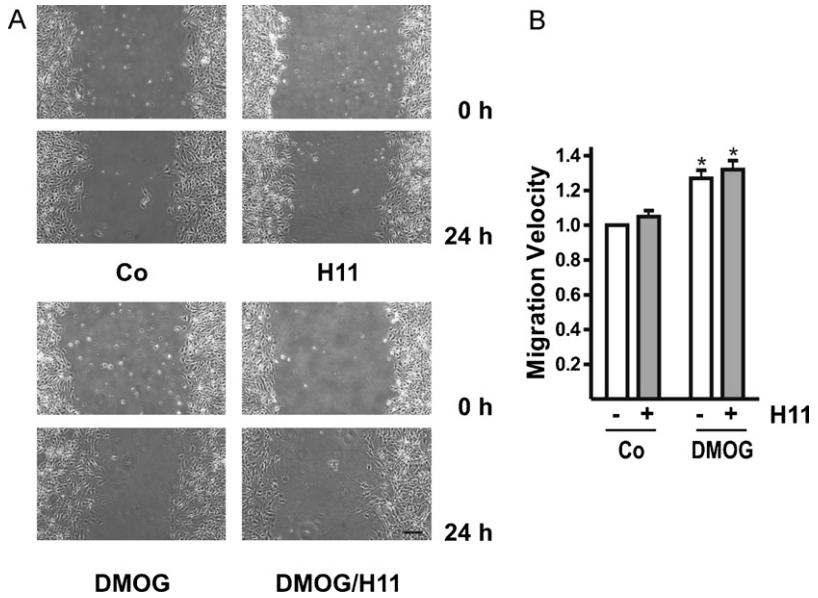

Fig. 2. Inhibition of Rho kinases does not affect lateral migration of glEND.2 cells. (A) glEND.2 cells were seeded around a barrier and allowed to become confluent. Upon removal of the barrier, cells were treated with DMOG (1 mM) or H1152 (1.5 μM) as indicated. Images were taken at the same positions at time 0 and 24 h. (B) Migration velocity was calculated by measuring the open space between the cell boundaries. Data of 4 independent experiments of cells migrating on glass or fibronectin are summarized in the graph. Migration velocity of control cells was set to 1. *Indicate significant ($p < 0.05$) differences compared to control cells.

inhibition of prolyl hydroxylases stabilizes hypoxia inducible factor and thus activates endothelial cells [37]. Treatment with DMOG only slightly stimulated migration velocity of the cells (about 25%, $n = 4$, $p < 0.05$ compared to control, Fig. 2B). The increase was independent of proliferation as DMOG decreased rather than increased proliferation of glEND.2 cells (data not shown). Surprisingly, incubation with the Rho kinase inhibitor H1152 did not significantly alter lateral migration of control cells or stimulated endothelial cells. Cells seeded on fibronectin migrated somewhat faster than cells on glass (data not shown) but treatment with H1152 and/or DMOG showed comparable effects (Fig. 2B).

The lateral migration assay was therefore not suitable to investigate ROCK-specific effects in glEND.2 cells, presumably because cell–matrix adhesion together with cell–cell adhesions were too strong and prevented sufficient movement of the cells.

3.3. Rho kinase inhibitors increase directional motility of endothelial cells from spheroids

In order to facilitate migration to a degree that would allow us to study ROCK-specific effects, glEND.2 cells were organized into spheroids over night and were then plated on glass plates coated with fibronectin. Approximately 2 h after adherence, cells started to migrate radially from the spheroids. Most of the cells remained attached to each other with only few cells loosing contact (Fig. 3A). Radial cohesive migration of endothelial cells from the spheroids was quantified by measuring the area covered by migrated cells, and the number of cells that have migrated away from the spheroid body (Fig. 3B). Incubation of spheroids with H1152 at the time of plating stimulated cell migration. A comparable increase was observed when the spheroids were plated on glass or on fibronectin, suggesting the effects of the Rho kinase inhibitor were largely independent of cell interaction with specific extracellular matrix proteins. We also confirmed by bromodeoxyuridine incorporation that the increase in cell numbers outside the spheroid body was not caused by H1152-induced proliferation of glEND.2 cells. Furthermore, increased migration was also observed even when cell division was inhibited by incubation with dichlorobenzimidazole riboside (DRB) (data not shown).

In order to further characterize cell movement, live cell imaging of cells migrating from spheroids was performed. Cells from 11 spheroids, 6 untreated controls and 5 after H1152 treatment, showed pronounced differences in their migration behavior (Fig. 4A/B). The mean square displacement of both untreated and treated cells followed a power-law in time (Fig. 4C). The MSD was larger for untreated cells at small time lags. At larger time lags, however, the MSD of the H1152-treated cells exceeded that of control cells (Fig. 4C) due to their larger power-law exponent (larger slope of the MSD, Fig. 4C inset). The differences in the MSD slope suggest that

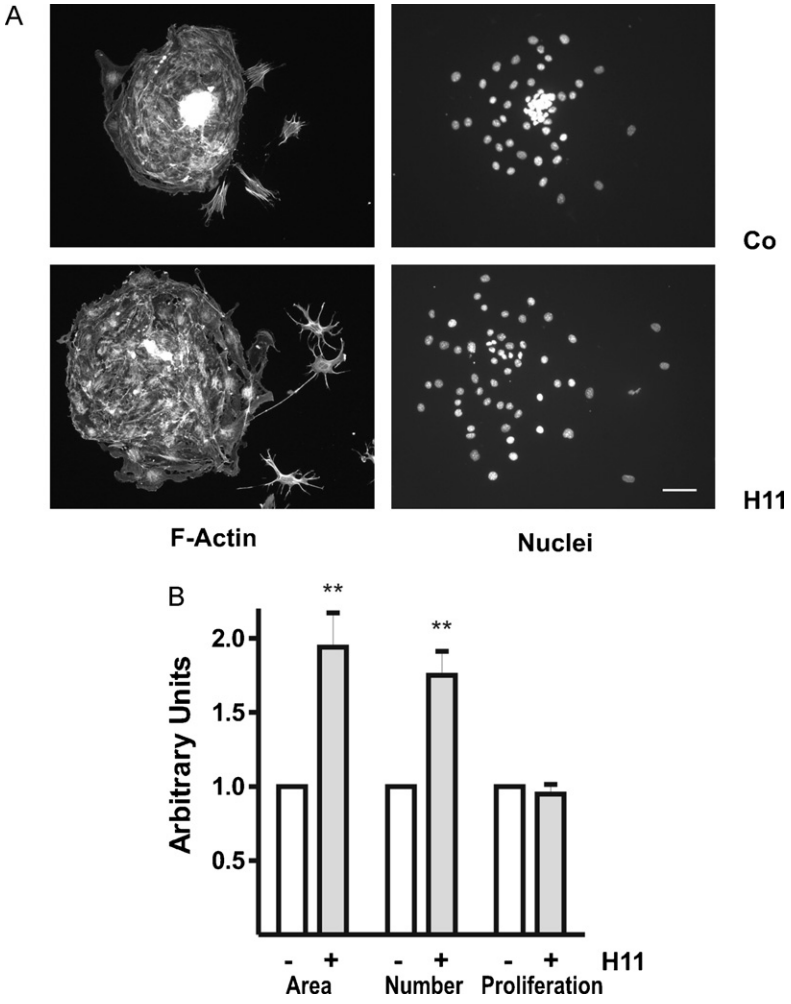

Fig. 3. Increased cell motility upon inhibition of Rho kinases. (A) Spheroids of endothelial cells were generated as described in Section 2. Upon plating on fibronectin-coated plates cells were treated with H1152 (1.5 μM). After 24 h F-actin fibers were visualized with rhodamine-phalloidin, and nuclei were stained with Hoechst. (B) For quantification purposes at least 6 spheroids were analyzed and the data of 3 independent experiments were summarized as means ± SEM, $^{**}p < 0.01$, two tailed one sample *t*-test. Proliferation was determined as ratio of BrdU-labeled cells to total cells.

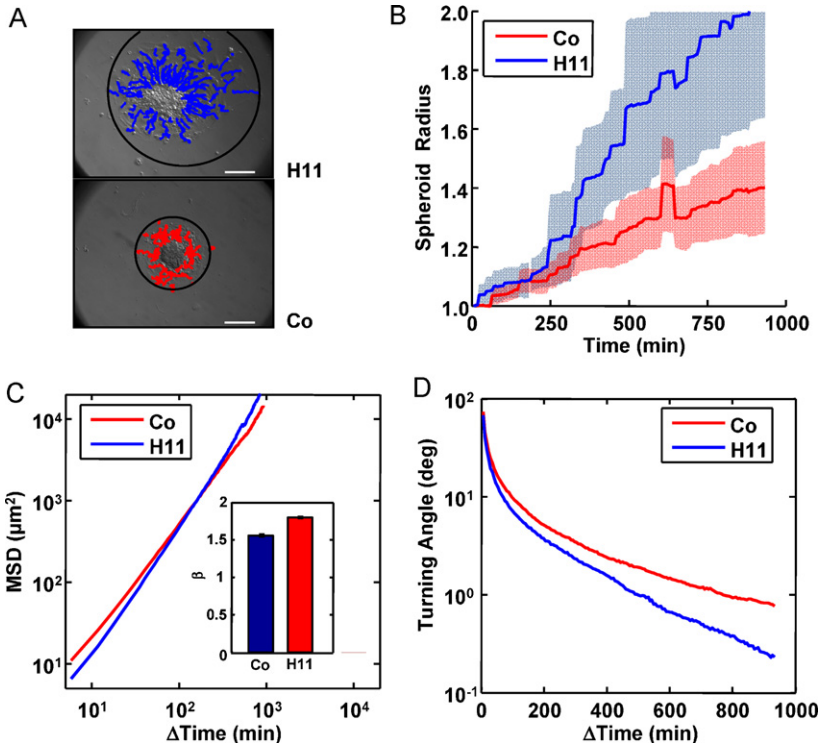

Fig. 4. Live cell imaging of spheroid migration. (A) Phase contrast images of spheroids and cell trajectories (red, control cells, blue H1152-treated cells) after 15 h. The smallest circle encompassing the cells is shown in black. Scale bar: 100 μm. (B) Average radius of the smallest circle enclosing all cells of a spheroid *versus* time, normalized to the spheroid radius at the beginning of the experiment. Data are mean values ± SEM (shown as shaded areas) of 665 control cells analyzed in 6 spheroids from 3 independent experiments, and 728 H1152-treated cells analyzed in 5 spheroids from 3 independent experiments. As the radius of the smallest circle is determined by a few cells at the periphery (B and C), the loss of cell trajectories *e.g.* during division can lead to sudden jumps in the curves. (C) Mean squared displacement (MSD) *versus* time in control cells (red, $n = 665$) and H1152-treated cells (blue, $n = 728$). The standard error of the geometric mean is smaller than the line width of the curves. Inset: power-law exponent β. (D) Average turning angle magnitude of H1152-treated and control cells at different time intervals. (For interpretation of the references to color in this figure legend, the reader is referred to the web version of the article.)

control cells moved more randomly, whereas H1152-treated cells moved more directionally persistent. This was confirmed by computing the turning angles of the cell trajectories as a function of the time lag (Fig. 4D). This difference in directional persistence of cell migration was mirrored by differences in cell shape. H1152-treated cells continuously changed their morphology by extending long protrusions that were absent or less pronounced in control cells (time lapse images, Supplementary Fig. 1).

3.4. Reorganization of proteins mediating cell–cell and cell–matrix interactions

Interference with RhoA–ROCK signaling altered the cytoskeletal architecture of the endothelial cells. Cell spanning F-actin stress fibers were reduced whereas the dense network of F-actin fibers below the nuclei remained unaltered. These changes were most obvious in leading cells and those, which separated from the coherent cells (Fig. 5A).

To address the possibility that cell–matrix interaction were reduced after ROCK inhibition, we analyzed Hic-5, a focal adhesion protein which has been shown to contribute to cell–matrix interactions in microvascular endothelial cells [38]. Hic-5 staining in focal adhesions was strongly reduced after ROCK inhibition in the leading cells of spheroids plated on fibronectin and also in cells that migrated as single cells, indicative of reduced interactions with the underlying matrix (Fig. 5A).

Inhibition of Rho kinases reduced cell–cell interactions leading to open gaps between the cells. Therefore, we tested whether Rho kinase inhibitors affected the expression or localization VE-cadherin, the major cell–cell adhesion molecule in endothelial cells. In control cells, VE-cadherin was detected at the cell–cell boundaries forming a rather uniform connection between neighboring cells (Fig. 5B). As cells separated upon treatment with H1152, VE-cadherin staining was interrupted. This reorganization, however, was not accompanied by a reduction of VE-cadherin expression. When analyzed by Western blotting, H1152-treated cells showed a tendency to higher rather than lower expression of VE-cadherin (Fig. 5C).

3.5. Role of ROCK2 in spheroid migration

Inhibition of ROCK2 activity after plating of the spheroids did not significantly increase the area covered by migrating cells (data not shown) but altered cell morphology toward a more irregular shape (Fig. 6A). Cells showed pronounced F-Actin lamellipodia, and cell to cell contacts were loosened. Individual cells separated and migrated extending long protrusions.

Downregulation of ROCK2 by siRNA did not impair the formation of spheroids. However, the size of the spheroids was reduced as determined by the area covered when spheroids attached 3 h after seeding (Fig. 6B). When corrected for the reduced spheroid size, the area covered by migrating cells was significantly increased (Fig. 6B). siRNA-treated cells lost F-actin bundles located below the lamellipodia, whereas lamellipodia stained strongly for F-actin (Fig. 6C). As shown for SLX2119-treated cells, tip cells separated more easily from the cells migrating as cohort.

3.6. Inhibition of Rho kinases increases endothelial cell motility in collagen-1 gels

Embedding of spheroids into collagen-1 gels is often used as a model system for vessel sprouting. In contrast to HUVEC,

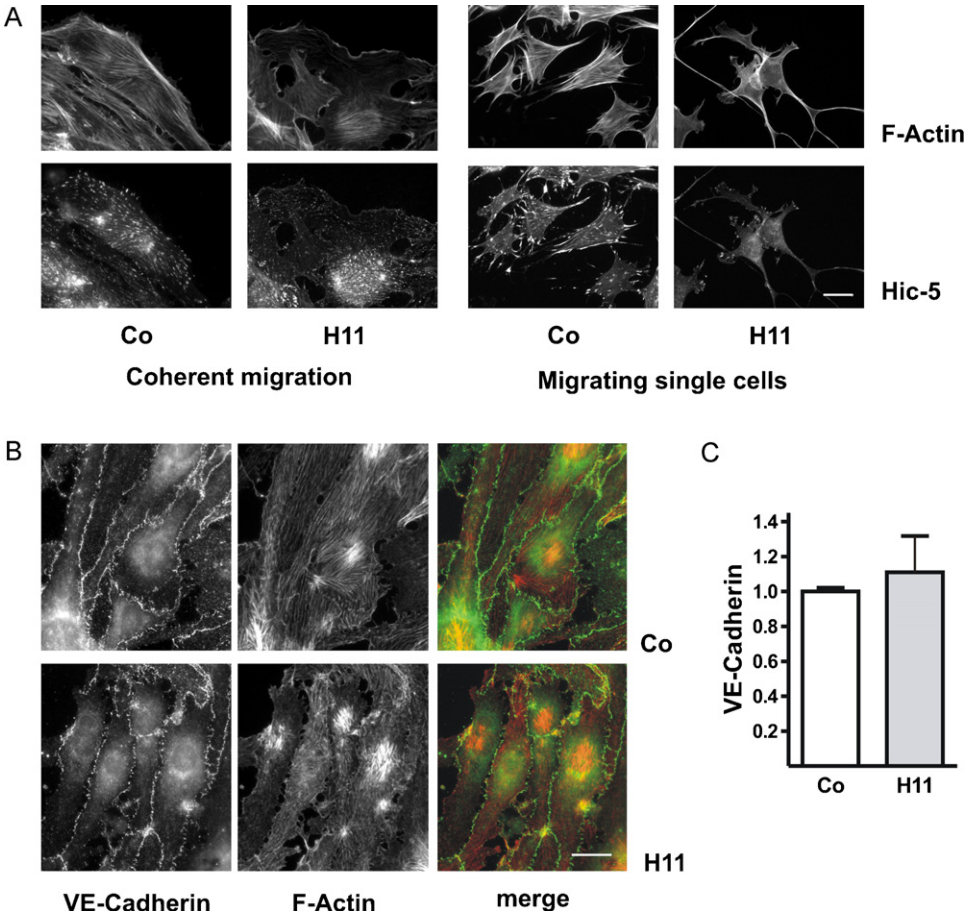

Fig. 5. Reorganization of proteins mediating cell–cell and cell–matrix interaction by Rho kinase inhibition. (A) glEND.2 cells were allowed to migrate from spheroids on fibronectin-coated plates for 24 h. Cells were stained for F-actin and the focal adhesion protein Hic-5. Scale bar: 30 μM. (B) VE cadherin and F-actin fibers were visualized in glEND.2 cells treated with H1152 (1.5 μM) for 24 h. (C) VE cadherin protein expression was analyzed in cells treated with H1152 (1.5 μM) for 24 h. Expression of VE cadherin was related to tubulin or vinculin expression, and normalized to control cells. Data are means ± SD of 3 independent experiments. Scale bar: 20 μM.

unstimulated glEND.2 spheroids did not show signs of sprouting in collagen-1 gels (Fig. 7A). After treatment of the spheroids with H1152 or SLX2119 for 2 days, however, single cells separated from the spheroid body and migrated radially into the gel.

Incubation of the spheroids with DMOG to induce VEGF and other growth factors resulted in sprout formation after 3 days of culture. This was observed with isolated spheroids and was further promoted by paracrine interactions between neighboring spheroids (Fig. 7B). Immunocytochemical analysis revealed a chain-like migration of endothelial cells rather than the formation vessel-like structures (Fig. 7B). When these spheroids were now treated for 24 h with H1152 or SLX2119, the number of chain-like sprouts was reduced (Fig. 7C). Cells lost contact with their neighbors (examples are indicated with arrows) and migrated as single cells. After prolonged incubation with the inhibitors for 2–3 days, the single cells started to reorganize into network-like structures (Fig. 7D) indicating that they were viable and functionally intact. Loss of contact and network formation was not observed in the absence of Rho kinase inhibitors where cells remained in a chain-like configuration.

4. Discussion

In this study we provide evidence that inhibition of Rho kinases favors structural alterations of microvascular endothelial cells and enhances their directional motility. Selective inhibition of ROCK2 mimicked the effect of non-selective Rho kinase inhibition but was less efficient in most assays.

Inhibition of Rho kinases reduced intracellular stress fibers without affecting the formation of lamellipodia in leading cells migrating off spheroids. Rho kinases stimulate actin-mediated contractility by increasing phosphorylation of myosin light chain, either by direct phosphorylation or more importantly by inhibiting myosin phosphatase [39]. Inhibition of Rho kinases, however, does not fully abolish contractility, because active MLC kinase (MLCK) may counteract Rho kinase inhibitors [40]. Inhibition of Rho kinases in microvascular glEND.2 cells reduced cellular stiffness and allowed the cells to alter their cell shape more easily best seen by time lapse imaging. Furthermore, cell to cell contacts were loosened, as demonstrated by the reduced cortical F-actin and the separation of the VE-cadherin-rich regions at cell–cell adhesions.

The change in motility after ROCK inhibition depended on the cellular microenvironment. When glEND.2 cells were plated on a stiff extracellular matrix such as coated glass, they adhered strongly to the substratum and formed tight bonds between cells. Under these conditions, inhibition of Rho kinases did not markedly alter cell migration. This finding may in part explain why Rho kinase inhibitors can be used in patients without severe side effects [41]. Endothelial cells in an intact vessel seem to be protected against disturbances of their cytoskeleton by Rho kinase inhibition at least in the absence of additional factors such as increased shear stress or injury.

In spheroid migration assays, newly formed cell–matrix interactions are essential for the movement of the cells. Comparing monolayer cultures and spheroid migration, Larsen et al. [42] observed coherent migration of carcinoma cells in a wound healing

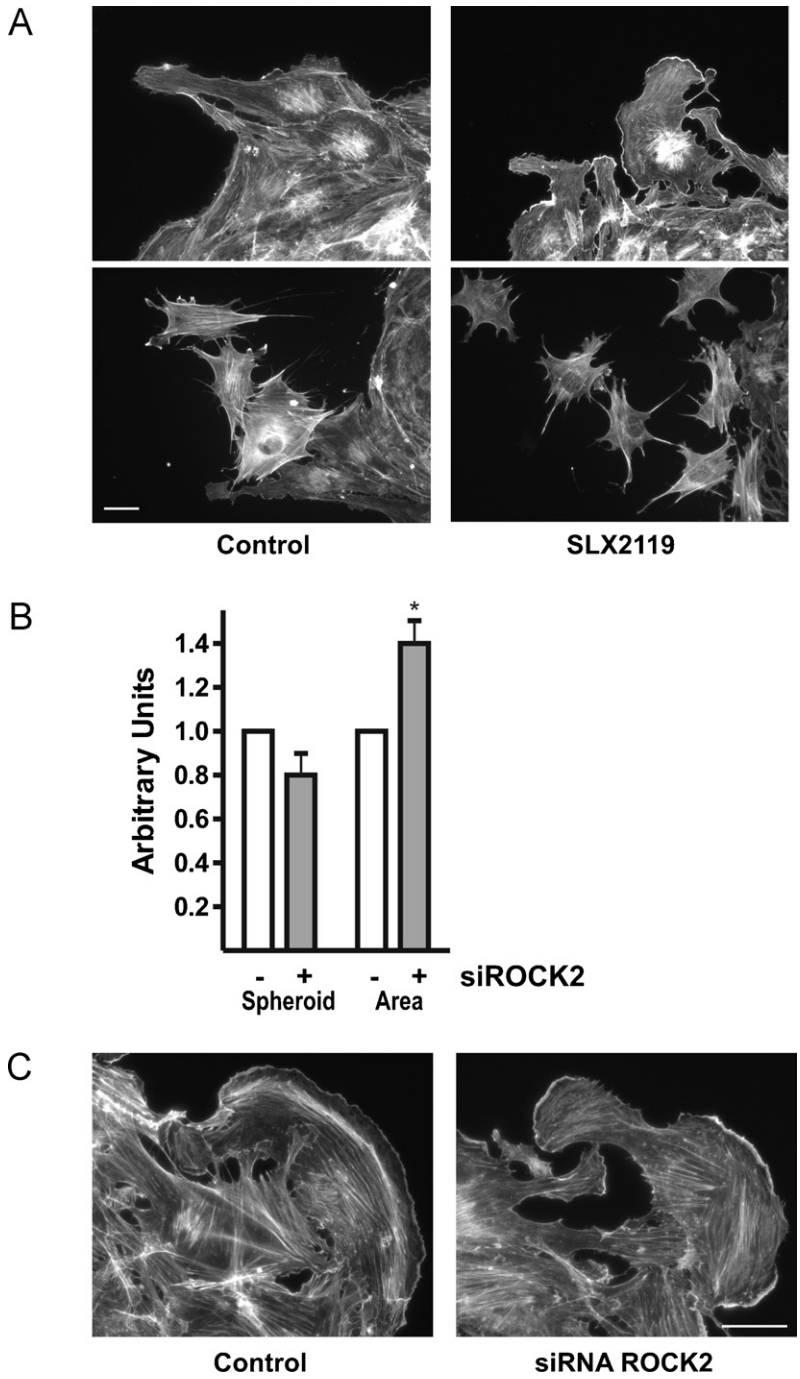

Fig. 6. Downregulation of ROCK2 facilitates endothelial cell movement. (A) Alterations of F-actin fibers by SLX2119 (1 μM) are shown in glEND.2 cells migrating from spheroids. Scale bar: 20 μM. (B) glEND.2 cells were treated with siRNAs during the period of spheroid formation. The area covered by the spheroid body was determined 3 h after plating und taken as a measure of spheroid size (spheroid). After 24 h, the area covered by migrating cells was determined and related to the area covered by the spheroids at 3 h (area). *Indicates significant ($p < 0.05$) differences, $n = 4$, 1 sample t-test. (C) Representative images of migrating endothelial cells stained for F-actin. Scale bar: 20 μM.

assay and formation of a scattered pattern upon movement from spheroids. In our experiments, glEND.2 cells that separated from the spheroid body migrated radially outward and formed circular monolayers. Upon Rho kinase inhibition, cell–cell contacts were loosened and the radial outward movement became more directionally persistent. Most strikingly, migrating single glEND.2 cells showed altered cell morphology in the presence of Rho kinase inhibitors with long extensions protruding into different directions. Spheroid migration thus represents an *in vitro* model system for flexible endothelial cells, which are loosely attached to each other and to the extracellular matrix and therefore resemble cells of newly forming vessels. In line with these findings, formation of tumor vessels has been shown to be interrupted by fasudil [43].

Our data from microvascular cells agree well with results from HUVEC or aortic endothelial cells that are derived from large vessel. Downregulation of RhoA–Rho kinase in these cells promoted cell spreading and cell migration [17,44]. Moreover, high levels of activated Rho kinase were reported to be important to stabilize established sprouts by stabilization of VE-cadherin through F-actin fibers [17,44].

The increased motility of endothelial cells after ROCK inhibition does not necessarily prevent network formation. After long term

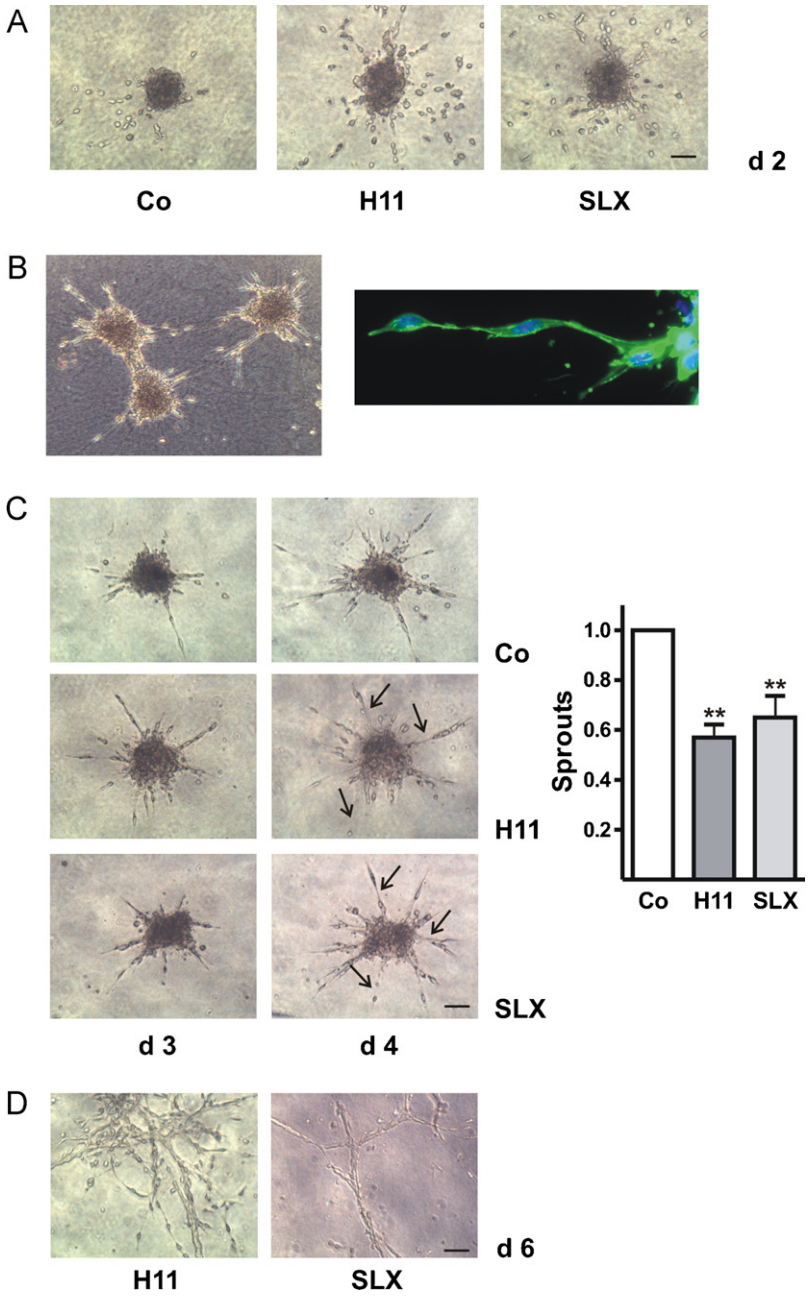

Fig. 7. Rho kinase inhibition interferes with chain migration of glEND.2 cells in collagen-1 gels. (A) Spheroids were embedded in collagen-1 gels and treated with H1152 (1.5 μM) or SLX2119 (1 μM). Photos were taken after 2 days and are representative of 3 independent experiments. Scale bar: 50 μM. (B) Spheroids were treated with 1 mM DMOG for 3 days to induce sprouting. To visualize cell structures cells were stained with rhodamine-phalloidin and Hoechst after fixation. (C) Individual spheroids without close neighbors were imaged 3 and 4 days after embedding in collagen gels. H1152 (0.75 μM) and SLX2119 (1 μM) were added at day 3 for 24 h. The number of intact sprouts of at least 7 spheroids was counted in 4 independent experiments. The number of sprouts was set to 1. Data are depicted as means ± SEM. The graph summarizes as means ± SEM; **Indicates significant ($p < 0.01$) differences compared to control. Scale bar: 50 μM. (D) Spheroids were cultured until day 6. At this time individual cells reorganized into structures. Representative data of cells treated with H1152 and SLX2119 are shown. Scale bar: 50 μM.

culture in collagen gels, glEND.2 cells with reduced Rho kinase activity formed networks of previously single cells. We speculate that the lower adhesiveness of the cells in the soft matrix allowed them to move and reorganize more readily. An earlier study that reported increased tube organization after Rho kinase inhibition with Y27632 in VEGF-stimulated human foreskin microvascular endothelial cells grown in a fibrin matrix also attributed their results to a lower adhesiveness [20]. Similarly increased cumulative sprout length was observed in VEGF-treated HUVEC upon incubation with H1152 [16].

In this study we also tested the effect of a selective inhibitor of the Rho kinase isoform ROCK2 as opposed to other inhibitors such as Y27632, hydroxyfasudil or H1152 that target both kinase isoforms and differ only in their inhibition profile against several other kinases [6]. Selectivity of Rho kinase inhibitors can easily be determined with purified enzymes, whereas the assessment of specificity in cellular systems is difficult because of the lack of specific substrates. Selectivity of SLX2119 has been reported to be 200-fold for ROCK2 over ROCK1 (IC50 105 nM for ROCK2 and 24 μM for ROCK1) [25]. In our cells, 1–2 μM SLX2119 was sufficient to inhibit phosphorylation of the direct substrate of Rho kinases, MYPT. Based on the analyses of Boerma et al. [25], these concentrations are unlikely to inhibit ROCK1.

The ROCK2 selective inhibitor SLX2119 has been reported to down-regulate CTGF in activated vascular smooth muscle cells isolated from human intestine with radiation-induced fibrosis [25], when the cells were incubated for 24 h with high concentrations of the inhibitor (40 μM), which were above the IC50 of ROCK1. In our experiments, short term inhibition of ROCK2 signaling by 1 μM SLX2119 was not sufficient to suppress LPA-mediated upregulation of CTGF even though the activity of Rho kinases was strongly inhibited as shown by impaired MYPT phosphorylation. Interestingly, we observed inhibition of CTGF induction when ROCK2 expression was reduced by siRNA. Specific binding proteins of ROCK2 have been described [45,46] and may contribute to the difference between inhibition of ROCK2 activity and reduced protein expression.

ROCK2 inhibition mimicked most but not all effects of the non-selective inhibitor H1152 as regards alterations of the cytoskeleton and alterations of cell motility, suggesting a predominant role of ROCK2 in endothelial cells. This notion is supported by the identification of ROCK2 as a mediator of LPA-induced expression of cell adhesion molecules in HUVECs [14]. Furthermore, ROCK2 plays a predominant role in regulating vascular contractility, as only ROCK2 can physically interacted with MYPT (=MBS, myosin binding subunit) [45]. However, in contrast to multiple *in vivo* studies, which have shown non-selective Rho kinase inhibitors as potential drugs for the treatment of various diseases, among them vascular diseases and atherosclerosis [5,8,10], *in vivo* data on the potential benefits of selective ROCK2 inhibitors is missing. ROCK2 −/− mice survive when generated in an appropriate background, but have not yet been tested in cardiovascular disease models [46]. Further *in vivo* studies are needed to clarify the role of ROCK2 as a potential therapeutic target.

Even though the basic molecular mechanisms of Rho kinase inhibitors are well established, the functional outcome of ROCK inhibition strongly depends on the cell type and the microenvironment. By comparing a wound healing and spheroid-collagen migration assays, we provide evidence that cellular responses to Rho kinase inhibition differ, depending on the model system used. Additional levels of complexity have to be considered when extrapolating from *in vitro* results to potential *in vivo* application of Rho kinase inhibitors as drugs. Microvascular endothelial cells differ from macrovascular endothelial cells in their phenotype (*e.g.* Ref. [47]). Whether they also differ in their response to ROCK inhibition is currently debated. Additional stimuli, which interfere with ROCK signaling pathways such as soluble mediators or mechanical stress can differ throughout the vasculature. *In vivo* experiments will be needed to analyze the impact of increased cellular flexibility and directional motility after ROCK inhibition.

In summary, inhibition of Rho kinases by non-selective inhibitors such as H1152 increases directed cellular motility and decreases cell–cell attachment of microvascular endothelial cells. Cell motility is also increased after inhibition of only one Rho kinase isoform, ROCK2, which suggests ROCK2 as potential drug target for controlling endothelial cell migration and structure formation.

Acknowledgments

This work was supported by the Interdisciplinary Center for Clinical Research (IZKF) at the University Hospital of the University of Erlangen-Nuremberg (project D5) and a grant from Deutsche Forschungsgemeinschaft. J.B. received a fellowship from the IZKF.

Appendix A. Supplementary data

Supplementary data associated with this article can be found, in the online version, at doi:10.1016/j.bcp.2011.12.012.

References

[1] Riento K, Ridley AJ. Rocks: multifunctional kinases in cell behaviour. Nat Rev Mol Cell Biol 2003;4:446–56.
[2] Prasain N, Stevens T. The actin cytoskeleton in endothelial cell phenotypes. Microvasc Res 2009;77:53–63.
[3] Miralles F, Posern G, Zaromytidou AI, Treisman R. Actin dynamics control SRF activity by regulation of its coactivator MAL. Cell 2003;113:329–42.
[4] Hahmann C, Schroeter T. Rho-kinase inhibitors as therapeutics: from pan inhibition to isoform selectivity. Cell Mol Life Sci 2010;67:171–7.
[5] Olson MF. Applications for ROCK kinase inhibition. Curr Opin Cell Biol 2008;20:242–8.
[6] Tamura M, Nakao H, Yoshizaki H, Shiratsuchi M, Shigyo H, Yamada H, et al. Development of specific Rho-kinase inhibitors and their clinical application. Biochim Biophys Acta 2005;1754:245–52.
[7] Asano T, Suzuki T, Tsuchiya M, Satoh S, Ikegaki I, Shibuya M, et al. Vasodilator actions of HA1077 in vitro and in vivo putatively mediated by the inhibition of protein kinase. Br J Pharmacol 1989;98:1091–100.
[8] Zhou Q, Gensch C, Liao JK. Rho-associated coiled-coil-forming kinases (ROCKs): potential targets for the treatment of atherosclerosis and vascular disease. Trends Pharmacol Sci 2011;32:167–73.
[9] Loirand G, Guerin P, Pacaud P. Rho kinases in cardiovascular physiology and pathophysiology. Circ Res 2006;98:322–34.
[10] Nunes KP, Rigsby CS, Webb RC. RhoA/Rho-kinase and vascular diseases: what is the link? Cell Mol Life Sci 2010;67:3823–36.
[11] Dong M, Yan BP, Liao JK, Lam YY, Yip GW, Yu CM. Rho-kinase inhibition: a novel therapeutic target for the treatment of cardiovascular diseases. Drug Discov Today 2010;15:622–9.
[12] Satoh K, Fukumoto Y, Shimokawa H. Rho-kinase: important new therapeutic target in cardiovascular diseases. Am J Physiol Heart Circ Physiol 2011;301: H287–96.
[13] Wolfrum S, Dendorfer A, Rikitake Y, Stalker TJ, Gong Y, Scalia R, et al. Inhibition of Rho-kinase leads to rapid activation of phosphatidylinositol 3-kinase/protein kinase Akt and cardiovascular protection. Arterioscler Thromb Vasc Biol 2004;24:1842–7.
[14] Shimada H, Rajagopalan LE. Rho kinase-2 activation in human endothelial cells drives lysophosphatidic acid-mediated expression of cell adhesion molecules via NF-kappaB p65. J Biol Chem 2010;285:12536–42.
[15] Venkatesh D, Fredette N, Rostama B, Tang Y, Vary CP, Liaw L, et al. RhoA-mediated signaling in notch-induced senescence-like growth arrest and endothelial barrier dysfunction. Arterioscler Thromb Vasc Biol 2011;31:876–82.
[16] Kroll J, Epting D, Kern K, Dietz CT, Feng Y, Hammes HP, et al. Inhibition of Rho-dependent kinases ROCK I/II activates VEGF-driven retinal neovascularization and sprouting angiogenesis. Am J Physiol Heart Circ Physiol 2009;296:H893–9.
[17] Mavria G, Vercoulen Y, Yeo M, Paterson H, Karasarides M, Marais R, et al. ERK-MAPK signaling opposes Rho-kinase to promote endothelial cell survival and sprouting during angiogenesis. Cancer Cell 2006;9:33–44.
[18] Yin L, Morishige K, Takahashi T, Hashimoto K, Ogata S, Tsutsumi S, et al. Fasudil inhibits vascular endothelial growth factor-induced angiogenesis in vitro and in vivo. Mol Cancer Ther 2007;6:1517–25.
[19] Hata Y, Miura M, Nakao S, Kawahara S, Kita T, Ishibashi T. Antiangiogenic properties of fasudil, a potent Rho-kinase inhibitor. Jpn J Ophthalmol 2008; 52:16–23.
[20] van Nieuw Amerongen GP, Koolwijk P, Versteilen A, van Hinsbergh VW. Involvement of RhoA/Rho kinase signaling in VEGF-induced endothelial cell migration and angiogenesis in vitro. Arterioscler Thromb Vasc Biol 2003;23:211–7.
[21] Yoneda A, Multhaupt HA, Couchman JR. The Rho kinases I and II regulate different aspects of myosin II activity. J Cell Biol 2005;170:443–53.
[22] Yoneda A, Ushakov D, Multhaupt HA, Couchman JR. Fibronectin matrix assembly requires distinct contributions from Rho kinases I and -II. Mol Biol Cell 2007;18:66–75.
[23] Lock FE, Hotchin NA. Distinct roles for ROCK1 and ROCK2 in the regulation of keratinocyte differentiation. PLoS One 2009;4:e8190.
[24] Bryan BA, Dennstedt E, Mitchell DC, Walshe TE, Noma K, Loureiro R, et al. RhoA/ROCK signaling is essential for multiple aspects of VEGF-mediated angiogenesis. FASEB J 2010;24:3186–95.
[25] Boerma M, Fu Q, Wang J, Loose DS, Bartolozzi A, Ellis JL, et al. Comparative gene expression profiling in three primary human cell lines after treatment with a novel inhibitor of Rho kinase or atorvastatin. Blood Coagul Fibrinolysis 2008;19:709–18.
[26] Li ZD, Bork JP, Krueger B, Patsenker E, Schulze-Krebs A, Hahn EG, et al. VEGF induces proliferation, migration, and TGF-beta1 expression in mouse glomerular endothelial cells via mitogen-activated protein kinase and phosphatidylinositol 3-kinase. Biochem Biophys Res Commun 2005;334:1049–60.
[27] Samarin J, Wessel J, Cicha I, Kroening S, Warnecke C, Goppelt-Struebe M. FOXO proteins mediate hypoxic induction of connective tissue growth factor (CTGF) in endothelial cells. J Biol Chem 2010;285:4328–36.
[28] Kroening S, Goppelt-Struebe M. Analysis of matrix-dependent cell migration with a barrier migration assay. Sci Signal 2010;3:pl1.
[29] Lin RZ, Chang HY. Recent advances in three-dimensional multicellular spheroid culture for biomedical research. Biotechnol J 2008;3:1172–84.
[30] Bursac P, Lenormand G, Fabry B, Oliver M, Weitz DA, Viasnoff V, et al. Cytoskeletal remodelling and slow dynamics in the living cell. Nat Mater 2005;4:557–61.
[31] Raupach C, Zitterbart DP, Mierke CT, Metzner C, Muller FA, Fabry B. Stress fluctuations and motion of cytoskeletal-bound markers. Phys Rev E Stat Nonlin Soft Matter Phys 2007;76:011918.

[32] Ikenoya M, Hidaka H, Hosoya T, Suzuki M, Yamamoto N, Sasaki Y. Inhibition of rho-kinase-induced myristoylated alanine-rich C kinase substrate (MARCKS) phosphorylation in human neuronal cells by H-1152, a novel and specific Rho-kinase inhibitor. J Neurochem 2002;81:9–16.
[33] Ott C, Iwanciw D, Graness A, Giehl K, Goppelt-Struebe M. Modulation of the expression of connective tissue growth factor by alterations of the cytoskeleton. J Biol Chem 2003;278:44305–11.
[34] Chaqour B, Goppelt-Struebe M. Mechanical regulation of the Cyr61/CCN1 and CTGF/CCN2 proteins. FEBS J 2006;273:3639–49.
[35] Muehlich S, Schneider N, Hinkmann F, Garlichs CD, Goppelt-Struebe M. Induction of connective tissue growth factor (CTGF) in human endothelial cells by lysophosphatidic acid, sphingosine-1-phosphate, and platelets. Atherosclerosis 2004;175:261–8.
[36] Kroening S, Stix J, Keller C, Streiff C, Goppelt-Struebe M. Matrix-independent stimulation of human tubular epithelial cell migration by Rho kinase inhibitors. J Cell Physiol 2010;223:703–12.
[37] Elvidge GP, Glenny L, Appelhoff RJ, Ratcliffe PJ, Ragoussis J, Gleadle JM. Concordant regulation of gene expression by hypoxia and 2-oxoglutarate-dependent dioxygenase inhibition: the role of HIF-1alpha. HIF-2alpha and other pathways J Biol Chem 2006;281:15215–26.
[38] Komorowsky C, Samarin J, Rehm M, Guidolin D, Goppelt-Struebe M. Hic-5 as a regulator of endothelial cell morphology and connective tissue growth factor gene expression. J Mol Med 2010;88:623–31.
[39] Kimura K, Itoh M, Amano M, Chihara K, Fukata Y, Nakafuku M, et al. Regulation of myosin phosphatatase by Rho and Rho-associated kinase (Rho-kinase). Science 1996;269:221–3.
[40] Kniazeva E, Putnam AJ. Endothelial cell traction and ECM density influence both capillary morphogenesis and maintenance in 3-D. Am J Physiol Cell Physiol 2009;297:C179–87.
[41] Suzuki Y, Shibuya M, Satoh S, Sugimoto Y, Takakura K. A postmarketing surveillance study of fasudil treatment after aneurysmal subarachnoid hemorrhage. Surg Neurol 2007;68:126–31.
[42] Larsen AB, Pedersen MW, Stockhausen MT, Grandal MV, van Deurs B, Poulsen HS. Activation of the EGFR gene target EphA2 inhibits epidermal growth factor-induced cancer cell motility. Mol Cancer Res 2007;5: 283–93.
[43] Nakabayashi H, Shimizu K. HA1077, a Rho kinase inhibitor, suppresses glioma-induced angiogenesis by targeting the Rho-ROCK and the mitogen-activated protein kinase kinase/extracellular signal-regulated kinase (MEK/ERK) signal pathways. Cancer Sci 2011;102:393–9.
[44] Varon C, Basoni C, Reuzeau E, Moreau V, Kramer IJ, Genot E. TGFbeta1-induced aortic endothelial morphogenesis requires signaling by small GTPases Rac1 and RhoA. Exp Cell Res 2006;312:3604–19.
[45] Wang Y, Zheng XR, Riddick N, Bryden M, Baur W, Zhang X, et al. ROCK isoform regulation of myosin phosphatase and contractility in vascular smooth muscle cells. Circ Res 2009;104:531–40.
[46] Shi J, Zhang L, Wei L. Rho-kinase in development and heart failure: insights from genetic models. Pediatr Cardiol 2011;32:297–304.
[47] Brouillet S, Hoffmann P, Benharouga M, Salomon A, Schaal JP, Feige JJ, et al. Molecular characterization of EG-VEGF-mediated angiogenesis: differential effects on microvascular and macrovascular endothelial cells. Mol Biol Cell 2010;21:2832–43.